PHYSICAL REVIEW A **95**, 021602(R) (2017)

Temperature-induced decay of persistent currents in a superfluid ultracold gas

A. Kumar, S. Eckel, F. Jendrzejewski, and G. K. Campbell*

Joint Quantum Institute, National Institute of Standards and Technology and University of Maryland, Gaithersburg, Maryland 20899, USA

(Received 21 July 2016; published 24 February 2017)

We study how temperature affects the lifetime of a quantized, persistent current state in a toroidal Bose-Einstein condensate. When the temperature is increased, we find a decrease in the persistent current lifetime. Comparing our measured decay rates to simple models of thermal activation and quantum tunneling, we do not find agreement. We also measured the size of the hysteresis loops in our superfluid ring as a function of temperature, enabling us to extract the critical velocity. The measured critical velocity is found to depend strongly on temperature, approaching the zero-temperature mean-field solution as the temperature is decreased. This indicates that an appropriate definition of critical velocity must incorporate the role of thermal fluctuations, something not explicitly contained in traditional theories.

DOI: 10.1103/PhysRevA.95.021602

Persistent currents invoke immense interest due to their long lifetimes, and they exist in a number of diverse systems, such as superconductors [1,2], liquid helium [3,4], dilute ultracold gases [5–7], and polariton condensates [8]. Superconductors in a multiply connected geometry exhibit quantization of the magnetic flux [9], while the persistent current states in a superfluid are quantized in units of $\hbar$, the reduced Planck constant. To create transitions between quantized persistent current states, the critical velocity of a superfluid (or critical current of a superconductor) must be exceeded. In ultracold gases, the critical velocity is typically computed at zero temperature, whereas experiments are obviously performed at nonzero temperature. In this Rapid Communication, we experimentally investigate the role of temperature in the decay of persistent currents in ultracold-atomic superfluid rings [Fig. 1(a)].

In the context of the free energy of the system, different persistent current states of the system (denoted by an integer ℓ, called the winding number) can be described by local energy minima, separated by energy barriers [here, we concentrate on $\ell = 0$ and $\ell = 1$ shown in Fig. 1(b)] [10,11]. The metastable behavior emerges from the energy barrier E_b between two persistent current states. For superconducting rings, the decay dynamics has been understood by the Caldeira-Leggett model [12]: The decay occurs either via quantum tunneling through the energy barrier or thermal activation over the top of the barrier. When first investigated in superconductors [13–19], the decay rate from the metastable state Γ was fit to an escape temperature $T_{\rm esc}$ by the relation $\Gamma = \Omega_a \exp(-E_b/k_B T_{\rm esc})$, where k_B is the Boltzmann constant. In the context of the Wentzel-Kramers-Brillouin (WKB) approximation in quantum mechanics or the Arrhenius equation in thermodynamics, Ω_a represents the "attempt frequency," i.e., how often the system attempts to overcome the barrier. The $\exp(-E_b/k_B T_{\rm esc})$ represents the probability of surmounting the barrier on any given attempt. The probability and thus the escape temperature in quantum tunneling is independent of temperature, while for thermal activation the escape temperature tracks the real temperature [Fig. 1(c)]. For our superfluid ring, the energy barrier E_b is much greater than all other energy scales in the problem, hence the lifetime of the persistent current is much greater than the experimental time scale. However, the height of the energy barrier and the relative depth of the two wells can be changed by the addition of a density perturbation [11]. The density perturbation may induce a persistent current decay even if its strength is less than the chemical potential [6,11].

Here, we measure the decay rate of a persistent current for various perturbation strengths and temperatures. We also measure the size of the hysteresis loops which (allows us to extract the critical velocity), showing a clear effect of temperature on the critical velocity in a superfluid.

The preferred theoretical tool for modeling atomic condensates is the Gross-Pitaevskii equation (GPE), which is a zero-temperature, mean-field theory. Recent experiments exploring the effect of rotating perturbations on the critical velocity of toroidal superfluids have found both agreement [21,22] and significant discrepancies [6,11] between experimental results and GP calculations. Several nonzero-temperature extensions to GP theory have been developed, including the Zaremba-Nikuni-Griffin (ZNG) formalism [23] and classical field [24] [of which the truncated Wigner approximation (TWA) is a special type]. To explore the role of temperature in phase slips in superfluid rings, Ref. [25] studied condensates confined to a periodic channel using TWA simulations. In addition, recent theoretical [26–32] and experimental [33] works explored a similar problem of dissipative vortex dynamics in a simply connected trap.

Our experiment consists of a ^{23}Na Bose-Einstein condensate (BEC) in a target-shaped optical dipole trap [34] [Fig. 1(a)]. The inner disk BEC has a measured Thomas-Fermi (TF) radius of 7.9(1) μm. The outer toroid has a Thomas-Fermi full width of 5.4(1) μm and a mean radius of 22.4(6) μm. To create the target potential, we image the pattern programed on a digital micromirror device (DMD) onto the atoms while illuminating it with blue-detuned light. This allows us to create arbitrary potentials for the atoms. Vertical confinement is created either using a red-detuned TEM_{00} or a blue-detuned TEM_{01} beam. The potential generated by the combination of the red-detuned TEM_{00} beam and ring beam is deeper than that of the blue-detuned TEM_{01} and ring beam, thus the temperature is generally higher in the red-detuned sheet potential. We use this feature to realize four different trapping configurations with temperatures T of 30(10), 40(12), 85(20),

*gcampbe1@umd.edu

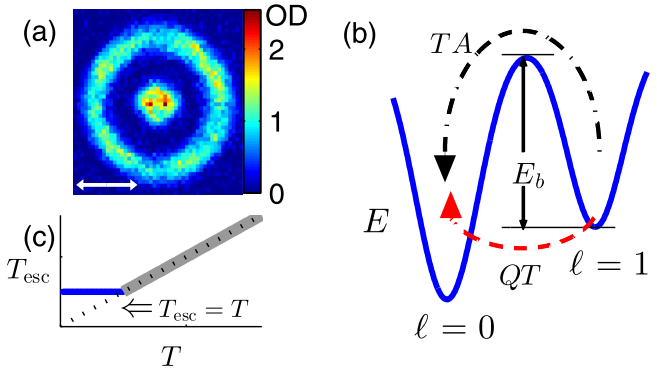

FIG. 1. Target-shaped condensate, energy landscape, and effective escape temperature. (a) *In situ* image of trapped atoms, with 5% of the total atoms imaged [20]. Experiments are performed on the ring-shaped BEC and the resulting winding number ℓ is read out by interfering the ring condensate with the disk-shaped BEC in time of flight. The disk-shaped BEC acts as a phase reference. (b) Energy landscape showing the stationary state, $\ell = 0$, and the persistent current state, $\ell = 1$, as minima in the potential. The energy barrier E_b needs to be overcome for a persistent current to decay from $\ell = 1$ to $\ell = 0$. The decay can be induced either via thermal activation (TA), or quantum tunneling (QT). (c) Crossover from quantum tunneling to the thermally activated regime. The escape temperature T_{esc} (see text) first remains constant (horizontal blue line) and then becomes equal to the physical temperature T (slanted gray line). A dotted line acts a guide to the eye depicting $T_{esc} = T$.

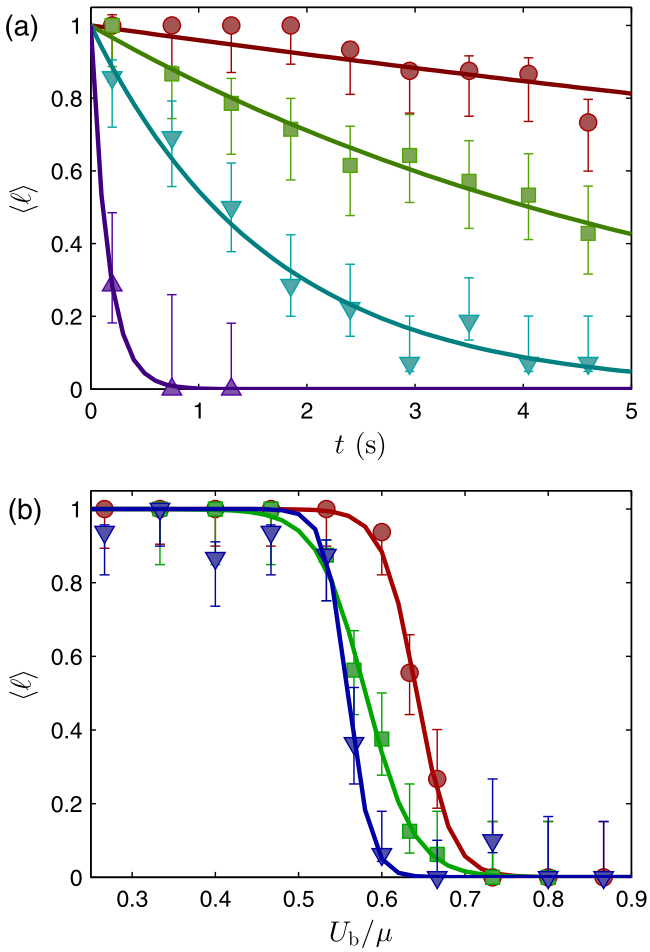

FIG. 2. (a) Average measured winding number $\langle \ell \rangle$ vs t, the duration for which a stationary perturbation is applied. The four data sets correspond to different strengths of the stationary perturbation U_b: 0.50(5)μ (circles), 0.53(5)μ (squares), 0.56(6)μ (inverted triangles), and 0.59(6)μ (triangles). Here, μ is the unperturbed chemical potential. The temperature of the superfluid was 85(20) nK. The solid curves show exponential fits. (b) The average measured winding number $\langle \ell \rangle$ vs U_b for fixed t: 0.5 s (circles), 2.5 s (squares), and 4.5 s (inverted triangles). The solid curves show a sigmoidal fit of the form $\langle \ell \rangle = \{\exp[(U_b/\mu - \zeta)/\alpha] + 1\}^{-1}$. The temperature of the superfluid was 40(12) nK.

and 195(30) nK, but all with roughly the same chemical potential of $\mu/\hbar = 2\pi \times [2.7(2)$ kHz]. (See the Supplemental Material [35] for details about temperature and trapping configurations.) Finally, a density perturbation is created by another blue-detuned Gaussian beam with a $1/e^2$ width of 6 μm and can be rotated or held stationary at an arbitrary angle in the plane of the trap [36].

To probe the lifetime of the persistent current, we first initialize the ring-shaped BEC into the $\ell = 1$ state with a fidelity of 0.96(2) (see Supplemental Material [35]). A stationary perturbation with a strength $U_b < \mu$ is then applied for a variable time t ranging from 0.2 to 4.6 s. To compensate for the 25(2) s lifetime of the condensate, we insert a variable length delay between the initialization step and application of the perturbation to keep the total time constant [without this normalization, a 25(2) s lifetime would cause an atom loss of $\approx$20% in 4.7 s, changing the chemical potential by $\approx$10%]. At the end of the experiment, the circulation state is measured by releasing the atoms and looking at the resulting interference pattern between the ring and disk BECs [11,37]. For each temperature, four different perturbation strengths are selected. The perturbation strengths are chosen such that the lifetime of the persistent current state is varied over the entire range of t. The measurement is repeated 16–18 times for each combination of U_b, T, and t. The average of the measured circulation states $\langle \ell \rangle$ gives the probability of the circulation state surviving for a given set of experimental parameters.

Figure 2(a) shows $\langle \ell \rangle$ vs t for $T = 85(20)$ nK and four different U_b. We fit the data to an exponential $\exp(-\Gamma t)$. GP theory predicts either a fast decay (<10 ms) or no decay, depending on the precise value of U_b/μ [25]. By contrast, we see from Fig. 2(a) that Γ changes smoothly from $4.1(6) \times 10^{-2}$ to 6.2(8) s^{-1} as U_b is changed from 0.50(4)μ to 0.59(5)μ. Thus we are able to tune the decay rate by over two orders of magnitude by changing the magnitude of perturbation by $\approx 0.1\mu$, in qualitative agreement with TWA simulation results [25]. This confirms that the decay of a persistent current is a probabilistic process, in contrast to the instantaneous, deterministic transitions seen in GPE simulations [25].

To explore whether a longer hold time shifts or broadens the transition between persistent current states, we measured the average persistent current as a function of U_b while keeping t constant. Figure 2(b) shows this measurement for three different t: 0.5, 2.5, and 4.5 s. We fit these data to a sigmoidal function of the form $\langle \ell \rangle = \{\exp[(U_b/\mu - \zeta)/\alpha] + 1\}^{-1}$ to extract estimates of the width α and center ζ of the transition [38]. We see that changing the perturbation strength by $\approx 0.2\mu$

decreases $\langle \ell \rangle$ from one to zero. The width α is essentially unchanged as we change t from 0.5 to 4.5 s, though the center of the sigmoid ζ shifts by $\approx 0.1 U_b/\mu$. We also took similar measurements at a temperature of 85(20) nK (not shown). The width α remains essentially independent of t even at higher temperatures. For a hold time $t = 0.5$ s, we found a center $\zeta = 0.50(4) U_b/\mu$ at $T = 85(20)$ nK; by contrast, we obtain $\zeta = 0.64(4) U_b/\mu$ for $T = 40(12)$ nK. This indicates that an increase in temperature makes a phase slip more probable, even with smaller U_b.

To understand if the decay of the persistent current is thermally activated or quantum mechanical in nature, we first must understand the nature of the energy barrier E_b that separates the two states. To estimate the size of E_b, we consider excitations that connect the $\ell = 1$ to the $\ell = 0$ state. In the context of a one-dimensional ring, a persistent current decay corresponds to having fluctuations reduce the local density, producing a soliton that subsequently causes a phase slip [39]. For rings with non-negligible radial extent, TWA simulations suggest that a vortex passing through the annulus of the ring (through the perturbation region) causes the transition [25]. Because of the narrow width of our ring, we expect that a solitonic vortex is the lowest-energy excitation that can connect two persistent current states [40–45]. An analytical form for the energy of a solitonic vortex is given by [41,42]

$$\epsilon_{\rm sv}(U_b/\mu) \approx \pi n_{\rm 2D} \frac{\hbar^2}{m} \ln\left(\frac{R_\perp}{\xi}\right) + \frac{1}{2} m N_c \left(\frac{\hbar}{2mR}\right)^2, \quad (1)$$

where N_c is the total number of condensate atoms in the ring, ξ is the healing length, $R_\perp$ is the Thomas-Fermi width of the perturbation region, and $n_{\rm 2D}$ is the maximum two-dimensional (2D) density in the region of the perturbation. The first term is the energy of a solitonic vortex while the second term is the kinetic energy of the remaining π phase winding around the ring. We note that N_c, $R_\perp$, ξ, and $n_{\rm 2D}$ all depend implicitly on T and U_b. Finally,

$$E_b(U_b, T) = \epsilon_{\rm sv} - \epsilon_{\ell=1} = \epsilon_{\rm sv} - \frac{1}{2} m N_c \left(\frac{\hbar}{mR}\right)^2, \quad (2)$$

where $\epsilon_{\ell=1}$ is the energy of the first persistent current state. We have verified the accuracy of these expressions using GP calculations similar to those in Refs. [41,42,46,47] to within 10% for our parameters.

Figure 3 shows the clear temperature dependence of the measured decay rate Γ of the persistent current. To quantify this dependence, we fit the data to the form $\Gamma = \Omega_a \exp(-E_b/kT_{\rm esc})$ for each temperature (shown as the solid lines in Fig. 3). We note that while the attempt frequency Ω_a is dependent on temperature [changing by five orders of magnitude from 40(12) nK to 195(30) nK], $T_{\rm esc}$ is not (see the inset of Fig. 3). In fact, $T_{\rm esc}$ is roughly constant at ≈ 3 μK, while the BEC temperature varies from 30(10) to 195(30) nK. The constancy of $T_{\rm esc}$ while real T is varied hints that a temperature-independent phenomenon sets the probability for tunneling on any given attempt. A similar effect was seen in superconductors [19], and is understood to be macroscopic quantum tunneling. We can estimate the decay rate due to quantum tunneling by drawing an analogy with an rf-superconducting quantum interference device. In this device, the quantum tunneling rate can be estimated by the WKB approximation $\Gamma_q \approx (\omega_p/2\pi)\exp(-E_b/\hbar\omega_p)$, where ω_p is the frequency of the first photon mode in the superconducting system [14]. Here, by analogy, ω_p is the frequency of the first azimuthal phonon mode, which is $\approx 2\pi \times 30$ Hz. For our system, $E_b/\hbar\omega_p > 10^3$, so $\Gamma_q \approx (\omega_p/2\pi)\exp(-10^3)$, implying that quantum tunneling should be negligible. Thus, the observed decay cannot be described by either simple thermal activation or quantum mechanical tunneling. It may be that more complicated models of energy dissipation may be required.

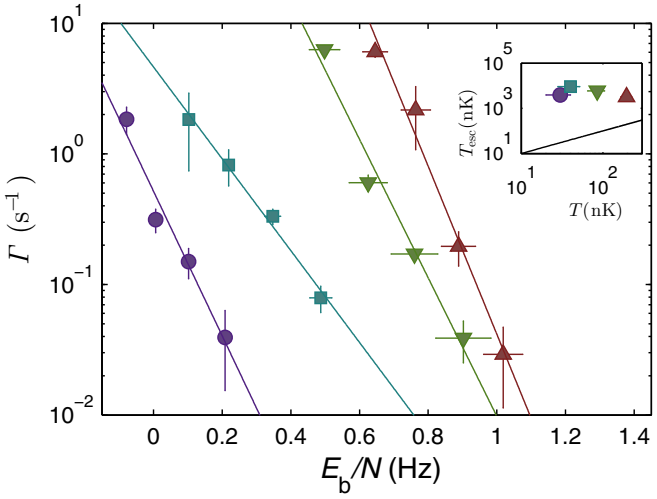

FIG. 3. Measured decay rate of the persistent current Γ as a function of perturbation strength U_b for four different temperatures: 30(10) nK (circles), 40(12) nK (squares), 85(20) nK (inverted circles), and 195(30) nK (triangles). The solid lines are fits of the form $\Gamma = \Omega_a \exp(-E_b/k_B T_{\rm esc})$, where E_b is the energy barrier, k_B is the Boltzmann constant, and $T_{\rm esc}$ and Ω_a are fit parameters. The inset shows the extracted $T_{\rm esc}$ as a function of measured physical temperature: 30(10) nK (triangle), 40(12) nK (square), 85(20) nK (circle), and 195(30) nK (inverted triangle). The solid line shows $T_{\rm esc} = T$.

Finally, because there are parallels between a vortex moving through the annulus of the ring and a vortex leaving a simply connected BEC, we investigated models that predict the dissipative dynamics of these vortices [30,32]. Such models predict lifetimes that scale algebraically with E_b and T. As can be seen from Fig. 3, our data scale exponentially with E_b. Thus, these models fail to explain the experimental data.

The measurements of the decay constants described above show the strong effect of temperature on the persistent current state. As discussed above, this temperature dependence is wholly captured in the variation of the constant Ω_a with T, as $T_{\rm esc}$ is constant. This causes an apparent change in the critical velocity of a moving barrier (for a given application time), with higher temperatures having lower critical velocities. Such a change in critical velocity affects hysteresis loops [11]. For an initial circulation state $\ell = 0(1)$, we experimentally determine $\Omega_+(\Omega_-)$, the angular velocity of the perturbation at which $\langle \ell \rangle = 0.5$. The hysteresis loop size is given by $\Omega_+ - \Omega_-$, normalized to Ω_0, where $\Omega_0 = \hbar/mR^2$, m is the mass of an atom, and R is the mean radius of the torus. We measure

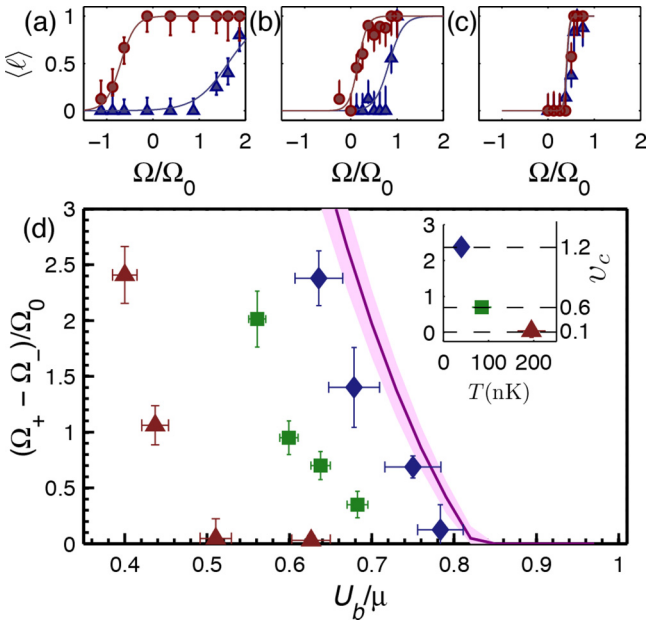

FIG. 4. Hysteresis loop for a perturbation strength of $0.64(4)U_b/\mu$ for (a) 40(12) nK, (b) 85(20) nK, and (c) 195(30) nK. (d) Size of the hysteresis loop $(\Omega_+ - \Omega_-)/\Omega_0$ (see text) vs barrier strength for three different temperatures: 40(12) nK (diamonds), 85(12) nK (squares), and 195(12) nK (triangles). The zero-temperature, GPE-predicted, area of the hysteresis loop is shown as a purple band, which incorporates the uncertainty in speed of sound. The left y axis of the inset shows the hysteresis loop size shown in (a)–(c) as a function of temperature for a perturbation strength of $0.64(4)U_b/\mu$. The numbers to the right show the corresponding extracted critical velocity v_c in (mm/s).

the hysteresis loop for four perturbation strengths and three different temperatures: 40(10), 85(20), and 195(30) nK, as shown in Fig. 4, with the zero-temperature GP prediction based on the speed of sound shown for Refs. [11,48]. We see from Fig. 4 that the discrepancy between experimental data and theoretical predictions decreases as the temperature is lowered. Using the density distribution of atoms around the ring, we extract the critical velocity from the hysteresis loop size [11]. For example, at $U_b/\mu = 0.64(4)$, a temperature change of 40(12) to 195(30) nK corresponds to a change in the critical velocity of $0.26(6)c_s$ to $0.03(2)c_s$. Here, c_s is the speed of sound in the bulk. While the measured critical velocity approached the zero-temperature speed of sound, we see that at nonzero temperature the thermal fluctuations must be taken into account in any measurement or calculation of the critical velocity.

In conclusion, we have measured the effect of temperature on transitions between persistent current states in a ring condensate in the presence of a local perturbation. The results of this work indicate that as thermal fluctuations become more pronounced, it becomes easier for the superfluid to overcome the energy barrier and the persistent current state to decay. If we assume that the decay is thermally driven and is thus described by an Arrhenius-type equation, we find a significant discrepancy between the measured temperature and the effective temperature governing the decay. Other possible mechanisms such as macroscopic quantum tunneling should be greatly suppressed. Despite the disagreement, we find a clear temperature dependence of the critical velocity of the superfluid by measuring hysteresis loops. This work will help to provide a benchmark for finite-temperature calculations on the decay of topological excitation in toroidal superfluids.

The authors thank M. Edwards, M. Davis, A. Yakimenko, and W. D. Phillips for useful discussions. This work was partially supported by ONR, the ARO atomtronics MURI, and the NSF through the PFC at the JQI.

[1] H. K. Onnes, Commun. Phys. Lab. Univ. Leiden 140c (May 1914), reprinted in Proc. K. Ned. Akad. Wet. **17**, 278 (1914).
[2] J. File and R. G. Mills, Phys. Rev. Lett. **10**, 93 (1963).
[3] J. B. Mehl and W. Zimmermann, Phys. Rev. **167**, 214 (1968).
[4] I. Rudnick, H. Kojima, W. Veith, and R. S. Kagiwada, Phys. Rev. Lett. **23**, 1220 (1969).
[5] C. Ryu, M. F. Andersen, P. Cladé, V. Natarajan, K. Helmerson, and W. D. Phillips, Phys. Rev. Lett. **99**, 260401 (2007).
[6] A. Ramanathan, K. C. Wright, S. R. Muniz, M. Zelan, W. T. Hill, C. J. Lobb, K. Helmerson, W. D. Phillips, and G. K. Campbell, Phys. Rev. Lett. **106**, 130401 (2011).
[7] S. Beattie, S. Moulder, R. J. Fletcher, and Z. Hadzibabic, Phys. Rev. Lett. **110**, 025301 (2013).
[8] D. Sanvitto, F. M. Marchetti, M. H. Szymańska, G. Tosi, M. Baudisch, F. P. Laussy, D. N. Krizhanovskii, M. S. Skolnick, L. Marrucci, A. Lemaître, J. Bloch, C. Tejedor, and L. Viña, Nat. Phys. **6**, 527 (2010).
[9] R. Doll and M. Näbauer, Phys. Rev. Lett. **7**, 51 (1961).
[10] E. J. Mueller, Phys. Rev. A **66**, 063603 (2002).
[11] S. Eckel, J. G. Lee, F. Jendrzejewski, N. Murray, C. W. Clark, C. J. Lobb, W. D. Phillips, M. Edwards, and G. K. Campbell, Nature (London) **506**, 200 (2014).
[12] A. Caldeira and A. Leggett, Ann. Phys. **149**, 374 (1983).
[13] J. M. Martinis, M. H. Devoret, and J. Clarke, Phys. Rev. Lett. **55**, 1543 (1985).
[14] J. Clarke, A. N. Cleland, M. H. Devoret, D. Esteve, and J. Martinis, Science **239**, 992 (1988).
[15] J. M. Martinis and H. Grabert, Phys. Rev. B **38**, 2371 (1988).
[16] R. Rouse, S. Han, and J. E. Lukens, Phys. Rev. Lett. **75**, 1614 (1995).
[17] D. B. Schwartz, B. Sen, C. N. Archie, and J. E. Lukens, Phys. Rev. Lett. **55**, 1547 (1985).
[18] F. Sharifi, J. L. Gavilano, and D. J. Van Harlingen, Phys. Rev. Lett. **61**, 742 (1988).
[19] R. F. Voss and R. A. Webb, Phys. Rev. Lett. **47**, 265 (1981).
[20] A. Ramanathan, S. R. Muniz, K. C. Wright, R. P. Anderson, W. D. Phillips, K. Helmerson, and G. K. Campbell, Rev. Sci. Instrum. **83**, 083119 (2012).

[21] F. Jendrzejewski, S. Eckel, N. Murray, C. Lanier, M. Edwards, C. J. Lobb, and G. K. Campbell, Phys. Rev. Lett. **113**, 045305 (2014).
[22] C. Ryu, P. W. Blackburn, A. A. Blinova, and M. G. Boshier, Phys. Rev. Lett. **111**, 205301 (2013).
[23] E. Zaremba, T. Nikuni, and A. Griffin, J. Low Temp. Phys. **116**, 277 (1999).
[24] P. Blakie, A. Bradley, M. Davis, R. Ballagh, and C. Gardiner, Adv. Phys. **57**, 363 (2008).
[25] A. C. Mathey, C. W. Clark, and L. Mathey, Phys. Rev. A **90**, 023604 (2014).
[26] S. J. Rooney, A. S. Bradley, and P. B. Blakie, Phys. Rev. A **81**, 023630 (2010).
[27] S. J. Rooney, A. J. Allen, U. Zülicke, N. P. Proukakis, and A. S. Bradley, Phys. Rev. A **93**, 063603 (2016).
[28] M. Kobayashi and M. Tsubota, Phys. Rev. Lett. **97**, 145301 (2006).
[29] B. Jackson, N. P. Proukakis, C. F. Barenghi, and E. Zaremba, Phys. Rev. A **79**, 053615 (2009).
[30] R. A. Duine, B. W. A. Leurs, and H. T. C. Stoof, Phys. Rev. A **69**, 053623 (2004).
[31] N. G. Berloff and A. J. Youd, Phys. Rev. Lett. **99**, 145301 (2007).
[32] P. O. Fedichev and G. V. Shlyapnikov, Phys. Rev. A **60**, R1779(R) (1999).
[33] G. Moon, W. J. Kwon, H. Lee, and Y.-i. Shin, Phys. Rev. A **92**, 051601 (2015).
[34] S. Eckel, F. Jendrzejewski, A. Kumar, C. J. Lobb, and G. K. Campbell, Phys. Rev. X **4**, 031052 (2014).
[35] See Supplemental Material at http://link.aps.org/supplemental/10.1103/PhysRevA.95.021602 for discussion of the experimental procedure, trapping configurations, temperature measurements, and the effect of non-zero temperature on the density perturbation calibration.
[36] K. C. Wright, R. B. Blakestad, C. J. Lobb, W. D. Phillips, and G. K. Campbell, Phys. Rev. Lett. **110**, 025302 (2013).
[37] L. Corman, L. Chomaz, T. Bienaimé, R. Desbuquois, C. Weitenberg, S. Nascimbène, J. Dalibard, and J. Beugnon, Phys. Rev. Lett. **113**, 135302 (2014).
[38] The extracted center and the full width at half maximum of the transition are independent of the form of the sigmoidal function chosen.
[39] W. A. Little, Phys. Rev. **156**, 396 (1967).
[40] J. Brand and W. P. Reinhardt, J. Phys. B **34**, L113 (2001).
[41] A. M. Mateo and J. Brand, New J. Phys. **17**, 125013 (2015).
[42] M. J. H. Ku, W. Ji, B. Mukherjee, E. Guardado-Sanchez, L. W. Cheuk, T. Yefsah, and M. W. Zwierlein, Phys. Rev. Lett. **113**, 065301 (2014).
[43] G. Valtolina, A. Burchianti, A. Amico, E. Neri, K. Xhani, J. A. Seman, A. Trombettoni, A. Smerzi, M. Zaccanti, M. Inguscio, and G. Roati, Science **350**, 1505 (2015).
[44] S. Donadello, S. Serafini, M. Tylutki, L. P. Pitaevskii, F. Dalfovo, G. Lamporesi, and G. Ferrari, Phys. Rev. Lett. **113**, 065302 (2014).
[45] M. Tylutki, S. Donadello, S. Serafini, L. P. Pitaevskii, F. Dalfovo, G. Lamporesi, and G. Ferrari, Eur. Phys. J.: Spec. Top. **224**, 577 (2015).
[46] J. Brand and W. P. Reinhardt, Phys. Rev. A **65**, 043612 (2002).
[47] S. Komineas and N. Papanicolaou, Phys. Rev. A **68**, 043617 (2003).
[48] G. Watanabe, F. Dalfovo, F. Piazza, L. P. Pitaevskii, and S. Stringari, Phys. Rev. A **80**, 053602 (2009).